The Mixing Layer Terrain Wind Adjustment Model (MILTWAM) for Airflow over Complex Terrain

S. A. Stage, Z. Wu, N. Mainkar, AND J. Weltman

Risk Management Division, Innovative Emergency Management Inc.

M. Myirski

Program Manager, Chemical Stockpile Emergency Preparedness, Aberdeen Proving Ground

May 3, 1999

8550 United Plaza Blvd, Baton Rouge, LA 70809
AND

5183 Blackhawk Road, Aberdeen Proving Ground, MD 21010

ABSTRACT

This paper presents the Mixing layer Terrain Wind Adjustment Model (MILTWAM) for airflow over complex terrain. MILTWAM is a diagnostic, mass-consistent, wind-field model based on NUATMOS (Ross, 1988). It is specifically designed for use in the D2-Puff dispersion model, and it produces realistic estimates of winds, even when only a few wind observations are available. This model is also fast enough for use in an emergency response dispersion model that runs on a personal computer (PC).

Several changes were made to the NUATMOS design to make MILTWAM suitable for this application:

1. The height of the top of the mixing layer is explicitly included in the model and imposes a non-porous upper lid on the flow. This upper lid is a major influence in determining the flow over the terrain.
2. A three-dimensional model with terrain-following coordinates is used when the top of the mixing layer is above the highest terrain; a vertically-averaged two-dimensional model is used when the mixing layer is below the highest terrain.
3. The winds output by the model are designed to agree with the observed winds at the observation points.

Model results are shown for simple geometric terrain and for real terrain. Winds produced by MILTWAM show greater variations in speed and direction than winds from NUATMOS.

1. Introduction

In the event of an accidental release of a hazardous chemical, emergency managers must be able to make rapid hazard assessments in order to recommend protective actions and protect the public welfare. Under sponsorship of the U. S. Army Chemical Stockpile Emergency Preparedness Program (CSEPP), Innovative Emergency Management (IEM) developed the D2-Puff dispersion model. The D2-Puff model is intended for use at the eight U. S. Army chemical stockpile sites, which store chemical munitions, and is designed to predict the dosages that would be received in the unlikely event of an accidental release of a chemical agent into the atmosphere. This paper describes the Mixing Layer Terrain Wind Adjustment Model (MILTWAM), the component of D2-Puff that computes wind fields over complex terrain.

Fast and reasonably accurate wind-field models are necessary for atmospheric dispersion models in order to predict the plume paths of atmospheric pollutants. The level of complexity of these wind-field models depends on the specific type of dispersion model for which they are being developed. MILTWAM produces mass-consistent flow, gives winds that agree with observations, produces realistic estimates of winds moving across terrain (even when only one wind observation or a few observations are used), and is fast enough for use in an emergency response dispersion model running on a personal computer (PC).

MILTWAM is a diagnostic model based on the NUATMOS model (Ross 1988). The influence of the depth of the mixing layer is included in MILTWAM. The model employs an additional technique that ensures that the adjusted winds agree with the observed winds used as model input. MILTWAM indicates that the terrain produces much larger variations in wind speed and direction than the variations indicated by NUATMOS.

Section 2 of this paper provides a brief background on models for winds that occur over complex terrain. Section 3 presents the equations and computational techniques used in MILTWAM, and section 4 discusses the differences between MILTWAM and the NUATMOS model. Section 5 shows a comparison of results from MILTWAM with analytic results for flow over geometrically shaped terrain. The series of figures in section 6 show the wind fields calculated for flow over the complex terrain surrounding the U.S. Army's Deseret Chemical Depot and illustrate the interaction of height of the mixing layer with the terrain in determining the flow pattern.

2. Background

Ratto *et al.* (1994) present a comprehensive review of kinematic models for wind fields over complex terrain. Kinematic models are also called mass-consistent models, although this name is somewhat misleading since dynamic models also conserve mass. Kinematic models are based solely on adjusting the observed wind field so that it satisfies the continuity equation. These models have been widely used in dispersion models and wind energy studies because they are computationally inexpensive and because they produce reasonably accurate results, even when little data is available. Kinematic models are purely diagnostic—they can not be used to make forecasts.

Dynamic models make use of the continuity equation and the momentum equation. They also generally include the equation of state and the thermodynamic equation. Dynamic models also sometimes include diabatic heating at the surface, radiative effects, and condensation and evaporation. These models estimate the time rate of change of atmospheric variables and can be used prognostically. Dynamic models include many physical processes that can not be directly

considered in kinematic models, like wave motions and thermal effects, such as sea breezes and drainage winds. Most dynamic models require data on the thermodynamic structure of the atmosphere. Dynamic models require more data and more computational time than kinematic models. Pennel (1983) and Burch and Ravenscroft (1992) found that simple kinematic models produce better wind fields than dynamic models in situations where critical data needed by the dynamic models are not available. Robe and Scire (1998) found that the California Meteorological Model (CALMET) kinematic model produced results that agreed with those from the MM5 dynamic model.

Because D2-Puff must run rapidly on a PC with limited data, MILTWAM was developed. MILTWAM is a kinematic model based on NUATMOS with some changes to make it more suitable for use in the situations for which D2-Puff was designed. The height of the mixing layer is included as an explicit model input parameter. The top of the mixing layer is assumed to be a non-porous surface; thus a closed, free-slip boundary condition is used. The resulting model produces much larger adjustments to the winds than NUATMOS and can lead to large differences between the winds used for model input and the model output at the same locations. This problem was corrected by including an algorithm that adjusts to achieve mass-consistent flow, but causes the model output winds to agree with the input at the observation locations. A more complete discussion of the differences between MILTWAM and NUATMOS is given in Section 4.

D2-Puff needs wind forecasts in order to forecast the location of the plume accurately. The Meso-Eta forecast model is currently routinely run twice a day for the contiguous United States with a grid spacing of about 20 km. The results are made available on the Internet. When forecast winds from this model or a similar model are available, they can be used as input to

MILTWAM. Draxler (1991) has shown that winds output by mesoscale dynamic models can be used in this way as input to a kinematic model. In this case, MILTWAM functions to interpolate the winds from the mesoscale model 20-km grid onto a 1-km grid in a manner that includes the effects of the local terrain. In other words, MILTWAM is used to adjust the winds from the mesoscale model to account for the effects of terrain at smaller scales than are considered by the mesoscale model.

Mesoscale model results with resolutions of 1 km will likely become available over the Internet within the next few years. If so, they should be considered for use in D2-Puff. However, it is not necessarily true that these more sophisticated models will increase the accuracy of the dispersion calculation (Draxler and Hess, 1998). Even if output from such a model is used, MILTWAM should remain in D2-Puff to ensure that dispersion calculations can be made for complex terrain at times when mesoscale model results cannot be obtained from the Internet.

3. The Mixing Layer Terrain Wind Adjustment Model (MILTWAM)

This section presents the equations used in MILTWAM.

a. Gridding the Winds

Let

$$\underset{l}{\vec{V}_{meas}} = \vec{V}_{meas}\left(\underset{l}{\vec{x}_{meas}}\right) \text{ for } l = 1, \mathrm{N}_{\mathrm{meas}} \tag{1}$$

be observations of wind vectors taken at various locations at a particular time. The first step in MILTWAM is to initialize a set of input wind vectors according to

$$\underset{l}{\vec{V}_{in}} = \underset{l}{\vec{V}_{meas}} \text{ for } l = 1, \mathrm{N}_{\mathrm{meas}} \tag{2}$$

Previous models do not use this step. The reasoning behind including this step in MILTWAM will be explained later, in *Preservation of Observations*.

The next step is to interpolate $\vec{V}_{in}$ onto the model computational grid using $1/r^2$ interpolation. The resulting gridded winds are denoted by $\vec{V}_0 = (u_0, v_0, w_0)$.

b. The Wind Adjustment Equations

Once the winds have been gridded, mass consistency is obtained by adjusting the winds. This technique makes use of the calculus of variations, as first suggested by Sasaki (1958). The difference between the gridded winds $\vec{V}_0 = (u_0, v_0, w_0)$ and the model output winds $\vec{V} = (u, v, w)$ is given by the functional

$$E(u, v, w) = \int \left[\alpha_1^2 (u - u_0)^2 + \alpha_1^2 (v - v_0)^2 + \alpha_2^2 (w - w_0)^2 \right] dV \qquad (3)$$

where α_1 and α_2 the Gaussian precision moduli.

The condition that the flow conserve mass is given by

$$H(x, y, z) = \vec{\nabla} \cdot \vec{V} = 0 \qquad (4)$$

The calculus of variations is used to minimize the difference between the input winds and the gridded winds, subject to the constraint that mass must be conserved. The Lagrange multiplier $\lambda(x, y, z)$ is used to produce the modified functional

$$F(x, y, z) = \int \left[\alpha_1^2 (u - u_0)^2 + \alpha_1^2 (v - v_0)^2 + \alpha_2^2 (w - w_0)^2 + \lambda \left(\frac{\partial u}{\partial x} + \frac{\partial v}{\partial y} + \frac{\partial w}{\partial z} \right) \right] dV \qquad (5)$$

The Euler-Lagrange equations are then

$$\frac{\partial \lambda}{\partial x} = 2\alpha_1^2 (u - u_0) \tag{6}$$

$$\frac{\partial \lambda}{\partial y} = 2\alpha_1^2 (v - v_0) \tag{7}$$

$$\frac{\partial \lambda}{\partial z} = 2\alpha_2^2 (w - w_0) \tag{8}$$

These three equations and equation (4) can be combined to get

$$\frac{\partial^2 \lambda}{\partial x^2} + \frac{\partial^2 \lambda}{\partial y^2} + \alpha^2 \frac{\partial^2 \lambda}{\partial z^2} = -2\vec{\nabla} \cdot \vec{V}_0 \tag{9}$$

where $\alpha = \frac{\alpha_1}{\alpha_2}$ and $\alpha_1 = 1$ is used without loss of generality. Equation (9) is a Poisson equation. Given sufficient boundary conditions, this equation can be solved to find λ.

Once λ is found, the adjusted model output winds are found using

$$u = u_0 + \frac{1}{2}\frac{\partial \lambda}{\partial x} \tag{10}$$

$$v = v_0 + \frac{1}{2}\frac{\partial \lambda}{\partial y} \tag{11}$$

$$w = w_0 + \frac{1}{2\alpha^2}\frac{\partial \lambda}{\partial z} \tag{12}$$

c. The Model Computational Grid

Properly specifying the terrain is a critical step in solving equation (9). If a Cartesian coordinate system is used, the terrain must be portrayed as a series of steps. Sherman (1978) used this implementation with fairly satisfactory results. However, Lewellen *et al*. (1982) showed that such a representation of the terrain led to an error of order 1 near the terrain surface. To work around this problem, Ross *et al.* (1988) used the terrain-following coordinates. This process involves the following co-ordinate transformation:

$$\tilde{x} = x \tag{13}$$

$$\tilde{y} = y \tag{14}$$

$$\sigma = \frac{z_t - z}{z_t - z_s(x, y)} = \frac{z_t - z}{\pi} \tag{15}$$

where z_t is the top of the computational box, $z_s(x, y)$ is the terrain function, and $\pi = z_t - z_s(x, y)$ is the thickness of the layer. This co-ordinate transformation results in transformed velocity components and the transformed Poisson equation, which are given as follows,

$$\tilde{u} = u \tag{16}$$

$$\tilde{v} = v \tag{17}$$

$$\tilde{w} = \frac{-1}{\pi}\left(w + \sigma u \frac{\partial \pi}{\partial x} + \sigma v \frac{\partial \pi}{\partial y} \right) \tag{18}$$

and

$$\begin{aligned} &\left(\frac{\partial}{\partial x} - \frac{\sigma}{\pi}\frac{\partial \pi}{\partial x}\frac{\partial}{\partial \sigma} \right)\left(\frac{\partial \lambda}{\partial x} - \frac{\sigma}{\pi}\frac{\partial \pi}{\partial x}\frac{\partial \lambda}{\partial \sigma} \right) + \\ &\left(\frac{\partial}{\partial y} - \frac{\sigma}{\pi}\frac{\partial \pi}{\partial y}\frac{\partial}{\partial \sigma} \right)\left(\frac{\partial \lambda}{\partial y} - \frac{\sigma}{\pi}\frac{\partial \pi}{\partial y}\frac{\partial \lambda}{\partial \sigma} \right) + \\ &\left(\frac{\alpha}{\pi} \right)^2 \frac{\partial^2 \lambda}{\partial \sigma^2} = -\frac{2}{\pi}\left(\frac{\partial \pi \tilde{u}_0}{\partial x} + \frac{\partial \pi \tilde{v}_0}{\partial y} + \frac{\partial \pi \tilde{w}_0}{\partial \sigma} \right) \end{aligned} \tag{19}$$

Equation (19) forms the basis of the NUATMOS model developed by Ross *et al.*

d. Boundary Conditions

Boundary conditions must be specified for λ on all of the boundaries of the model domain. The Neumann boundary condition states that $\frac{\partial \lambda}{\partial \hat{n}} = 0$, where $\hat{n}$ is the direction normal to the boundary. The Neuman boundary condition is a closed boundary condition because it states that the velocity perpendicular to the boundary is not adjusted, and that therefore the mass flux across the boundary in the model output winds is the same as in the gridded winds. Note that there can be an adjustment in the component of the winds tangential to the boundary, so the Neumann boundary condition can be called a closed free-slip boundary condition.

The Dirichlet boundary condition states that $\lambda = 0$ on the boundary. In this case, the tangential component of the model output winds at the boundary are equal to the tangential component of the gridded winds. There is an adjustment in the normal component of the velocity and thus in the flow of mass across the boundary. The Dirichlet boundary condition can be called an open boundary condition.

Open boundary conditions are used at the lateral sides of the model domain. The closed free slip boundary condition is used at the surface of the earth. MILTWAM uses the top of the mixing layer for the top model level, z_t, and applies a closed free slip boundary condition there. As discussed later in *Discussion of Differences between MILTWAM and NUATMOS*, this is a significant departure from NUATMOS (Ross *et al.*, 1988, 1993).

e. Cases when the Mixing Layer Top Intersects the Terrain

At CSEPP sites, the top of the mixing layer is often below the tops of the highest terrain, indicating that the air flow is confined to low lying basins and valleys. The terrain-following coordinate system can not be used in this case because the thickness of the mixing layer becomes zero over the peaks, and equation (15) can not be used. It would be possible to include internal boundaries within the model domain along the curves where the surface and the top of the mixing layer intersect, and include appropriate boundary conditions there. However, a simpler approach, which is computationally much faster and gives acceptable flows, was chosen for use in MILTWAM.

MILTWAM uses a two-dimensional model for cases when the top of the mixing layer is below the highest terrain in the domain. This model is obtained by vertically averaging the winds from the surface to the top of the mixing layer and then following steps similar to those used to develop the three-dimensional part of the model.

The layer-averaged wind components are given by

$$\bar{u}(x,y) = \frac{1}{\pi(x,y)} \int_{z_s(x,y)}^{z_t} u(x,y,z)\,dz \tag{20}$$

$$\bar{v}(x,y) = \frac{1}{\pi(x,y)} \int_{z_s(x,y)}^{z_t} v(x,y,z)\,dz \tag{21}$$

Equations (20) and (21) can be used in equation (3) to get

$$E(u,v) = \int \pi^2 \left[(\bar{u} - \bar{u}_0)^2 + (\bar{v} - \bar{v}_0)^2 \right] dx\,dy \tag{22}$$

which is the functional to be minimized.

Equation (4) becomes

$$H(x,y) = \vec{\nabla}_H \cdot (\pi \vec{V}) = 0 \tag{23}$$

which is the strong constraint associated with mass conservation.

In this case, $\vec{\nabla}_H = \left(\frac{\partial}{\partial x}, \frac{\partial}{\partial y}, 0 \right)$ is the horizontal gradient operator.

After introducing Lagrange multipliers $\lambda(x,y,z)$, the modified functional becomes

$$F(x,y) = \int \left[\pi^2 (\bar{u} - \bar{u}_0)^2 + \pi^2 (\bar{v} - \bar{v}_0)^2 + \lambda \left(\frac{\partial(\pi\bar{u})}{\partial x} + \frac{\partial(\pi\bar{v})}{\partial y} \right) \right] dxdy \tag{24}$$

The Euler-Lagrange equations in terms of the generalized coordinates $\bar{u}$ and $\bar{v}$ are then

$$\frac{\partial \lambda}{\partial x} = 2\pi(\bar{u} - \bar{u}_0) \tag{25}$$

$$\frac{\partial \lambda}{\partial y} = 2\pi(\bar{v} - \bar{v}_0) \tag{26}$$

Using equations (25), (26), and (23), one can show that

$$\frac{\partial^2 \lambda}{\partial x^2} + \frac{\partial^2 \lambda}{\partial y^2} = -2\vec{\nabla} \cdot (\pi \vec{V}_0) \tag{27}$$

Thus, the Poisson equation for the case when the mixing-layer intersects the terrain appears very similar to the equation for the case involving a mixing-layer above the terrain, except that the entire terrain dependence is contained in the source term on the right-hand side. Also, since the *z*-dependence has been removed from the equations, the entire transformation to

terrain-following coordinates is circumvented and the equations are able to handle the cases for which the boundary layer intersects the terrain.

The layer-mean winds are found from λ using

$$\bar{u} = \bar{u}_0 + \frac{1}{2\pi}\frac{\partial \lambda}{\partial x} \tag{28}$$

$$\bar{v} = \bar{v}_0 + \frac{1}{2\pi}\frac{\partial \lambda}{\partial y} \tag{29}$$

The two-dimensional part of the model requires that all of the adjustment be in the horizontal component of the winds. This is equivalent to using $\alpha \to \infty$ in the three-dimensional part of the model.

f. The Parameter α

The parameter α, which determines the relative amounts of horizontal and vertical adjustment, was quite important in previous wind adjustment models, and has received considerable discussion in related literature (Ratto *et al.*, 1994). In MILTWAM, the height of the mixing layer is the dominant factor in limiting vertical adjustment, and α is much less important. As will be seen later in *Results for Real Terrain*, the height of the mixing layer is often below the top of the terrain at CSEPP sites. In this case, MILTWAM uses the two-dimensional model equations, and α is not used.

When the top of the mixing layer is above the highest terrain, the three-dimensional equations are used, as well as α. However, tests show that the results are not very sensitive to the value of α. When the top of the mixing layer is only slightly above the highest terrain, the lid at

the top of the mixing layer still effectively suppresses the vertical motions and the value of α does not make a significant difference. When the height of the mixing layer is farther above the terrain, the wind adjustments are small, and α does not have much impact on the flow. The value of α^2 for the Deseret Chemical Depot was subjectively determined to be 1.0 for Pasquill stabilities A, B, and C, 0.31 for Pasquill stability D and E, and 0.031 for Pasquill stability F.

g. Preservation of Observations

MILTWAM produces much larger adjustments to the winds than NUATMOS. If these adjustments were left uncorrected, they would sometimes lead to large differences between the observed winds used as model input and the adjusted model output winds at the observation locations. The wind directions can differ by more than 90 degrees, which would place the chemical plume in the wrong location. This unacceptable behavior arises because the functional in equation (3) minimizes the difference between the gridded data and the model output rather than the difference between the observations and the model output. This occurrence was not a serious problem in NUATMOS since it produces small adjustments.

MILTWAM uses an algorithm specifically designed to satisfy mass conservation, but also to ensure that the model output winds agree with the observed input winds at the observation locations. Let

$$\vec{V}_{out_l} = \vec{V}\left(\vec{x}_{meas_l} \right) \text{ for } l = 1, \mathrm{N}_{\mathrm{meas}} \tag{30}$$

In other words, interpolate from the model results on the grid to find the model output winds at the observation points. These output winds are a function of the input winds, namely

$$\vec{V}_{\underset{l}{out}} = \mathrm{F}\left(\vec{V}_{\underset{m}{in}} \right) \text{ for } l = 1, \mathrm{N}_{\text{meas}} \text{ and } m = 1, \mathrm{N}_{\text{meas}} \tag{31}$$

where $\mathrm{F}(\ )$ indicates the entire process of applying the MILTWAM model equations to find the model output winds at the observation points. In general, $\vec{V}_{\underset{l}{out}} \neq \vec{V}_{\underset{l}{meas}}$. MILTWAM uses an interactive technique to adjust $\vec{V}_{\underset{l}{in}}$ until $\vec{V}_{\underset{l}{out}} = \vec{V}_{\underset{l}{meas}}$. The iteration technique uses a secant method (Press *et al*., 1977).

h. Solution Algorithm

MILTWAM solves equation (19) by using a multi-grid method (Briggs, 1987). The model domain has a horizontal extent of 97 by 97 km, with a horizontal grid spacing of 1 km. Three full multi-grid cycles, each consisting of six different grid sizes, are used. The equations presented in *Preservation of Observations* are applied after each of the first two cycles to ensure agreement between the model output and the observations. Then one additional multi-grid cycle is run to get final convergence of the mass conservation adjustment. The three-dimensional part of the model runs with five evenly spaced vertical levels, while the two-dimensional part of the model has one vertical level.

This method produces accurate solutions to the model equations. It is also extremely fast—the multi-grid method is approximately one hundred times faster than the simple over relaxation (SOR) algorithm. The wind field for a set of wind observations at one observation time can be found in less than five seconds on a 166 MHz Pentium PC.

4. Discussion of Differences between MILTWAM and NUATMOS

As stated above, MITLWAM is based on NUATMOS, but incorporates several changes that make it more suitable for use in the D2-Puff dispersion model. Important differences between the two models are the upper boundary condition, the sense in which the models can be said to agree with the observed winds, and the role played by the parameter α. These correspond to somewhat different assumptions about the physics that govern the flow.

NUATMOS uses an open boundary condition at the top of the model domain and must use a computational grid with the top layer well above the highest terrain feature. This is equivalent to saying that air is free to flow across the upper boundary of the model. The model parameter α determines the relative amount of vertical and horizontal adjustment in the flow (see Ratto, *et al.* 1994 for a discussion of the role of α in NUATMOS and other kinematic models). Smaller values of α are used to reflect the suppression of vertical motions in stable situations, while larger values are used in unstable cases. NUATMOS does not include any explicit consideration of the effect of the depth of the mixing layer on the flow.

MILTWAM is based on the physical assumption that the top of the mixing layer acts like a non-porous material surface and restricts vertical motion. This is implemented in the model by a closed free slip upper boundary condition. The assumption is that the dominant physical process over complex terrain is that the airflow is trapped between the surface and the top of the mixing layer and that the flow must conserve mass while agreeing with the observations. The winds are therefore modeled by potential flow between the surface of the earth and the top of the mixing layer. The effects of atmospheric stability then enter indirectly by way of their influence

on the mixing layer depth. Although the parameter α appears in the 3D equations in MILTWAM, it plays a minor role and does not much effect model results.

The top of the mixing layer is often below the highest terrain. In this case MILTWAM uses a 2D potential flow for the mixing layer. The flow is either deflected around or blocked by the protruding terrain, but the air is prevented from flowing over the top of terrain that is above the top of the mixing layer.

The goal of NUATMOS is to make small adjustments to the flow to obtain a mass-conserving flow. NUATMOS requires a large number of wind observations so that the gridded winds capture the main features of the flow. Although the NUATMOS model accepts even a single wind observation, in practice, it has always been used with at least 10 meteorological readings at different locations. The model then makes small adjustments to remove divergence. In Ross *et al.* (1988) the model is considered successful, in part, because the adjustment is small, *i.e.*, the difference between the gridded and adjusted winds is small. The streamlines show little deflection around terrain unless the observations have sufficient density to resolve the deflection.

The goal of MILTWAM is to adjust the wind field to flow around the terrain in a mass-consistent manner. The output must agree with the observations, but the adjustments at other locations can be large if required by the terrain. MILTWAM produces much larger adjustments in the wind field than NUATMOS. The streamlines tend to follow the terrain, even when only one or a few observations are used.

5. Model Testing

MILTWAM was tested by using three simple geometrically shaped terrain for which classical potential flow solutions exist:

- a hemisphere
- a half cylinder
- a cylinder.

a. Test Case 1: Hemispherical Mountain

The first test case for geometric terrain is a hemispherical mountain with a radius of 6 km. The computational grid is 49 by 49 km, with a grid spacing of 1 km. The model top is set to 21 km, with 100 layers. An open boundary condition is used at the top so that the results could be compared with the analytic solution. The free-stream speed is 1 m/s in the x-direction.

Figure 1 shows the near-surface wind speed as a function of along wind distance from the center of the peak. MILTWAM speed at the top of the hemisphere is 1.51 m/s, which is very close to the analytic solution of 1.5 m/s. The speed at the stagnation point is 0.4 m/s, as compared to zero for the analytic case. At distances beyond 8 km, MILTWAM and the analytic solution closely agree. Figure 2 shows the speed as a function of cross-wind distance from the center of the peak. The simulation results agree fairly well with the analytic curve, and the difference between the two curves differs by a maximum of 21% at a distance of 6 km from the center. Similarly, Figure 3 shows the vertical wind speed as a function of distance above the top of the peak. The agreement between the model results and the analytic solution is excellent throughout.

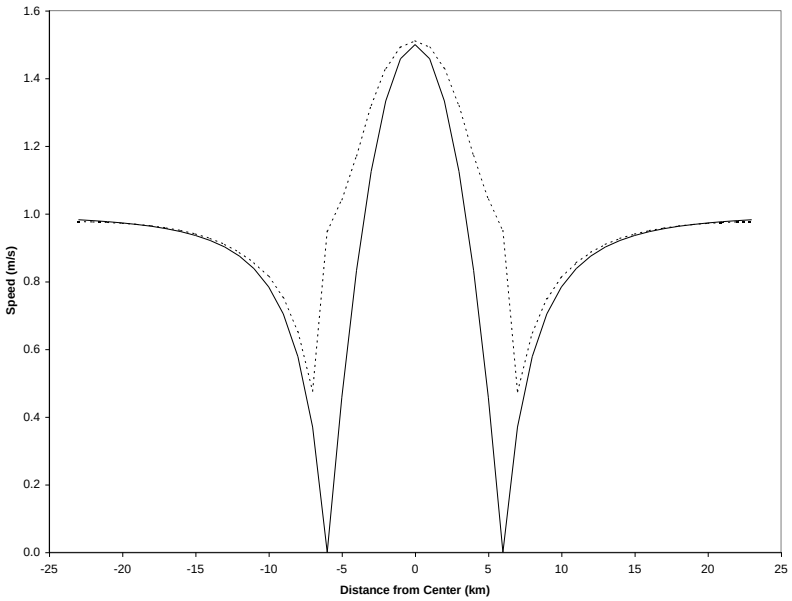

Figure 1: Surface wind speed over a hemispherical mountain as a function of along wind distance. (MILTWAM results are dotted. Analytic solution results are solid.)

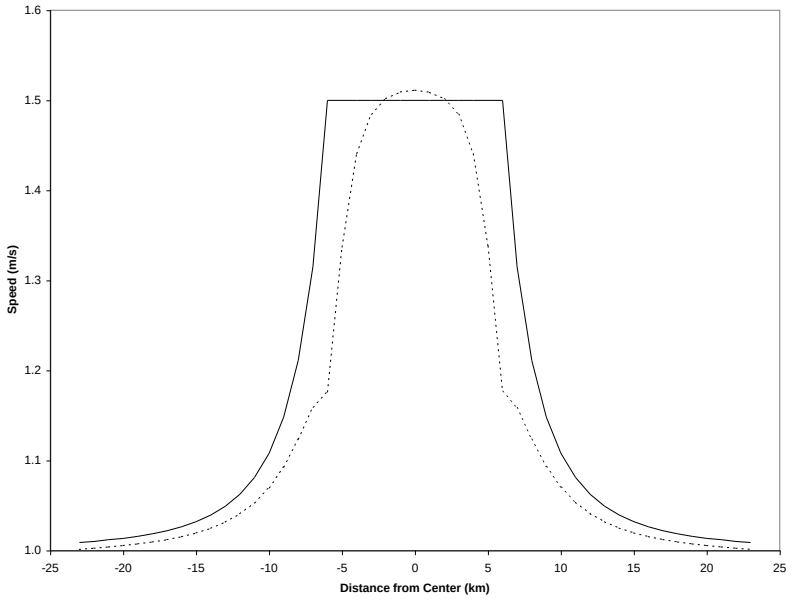

Figure 2: Surface wind speed over a hemispherical mountain as a function of cross-wind distance. (MILTWAM results are dotted. Analytic solution results are solid.)

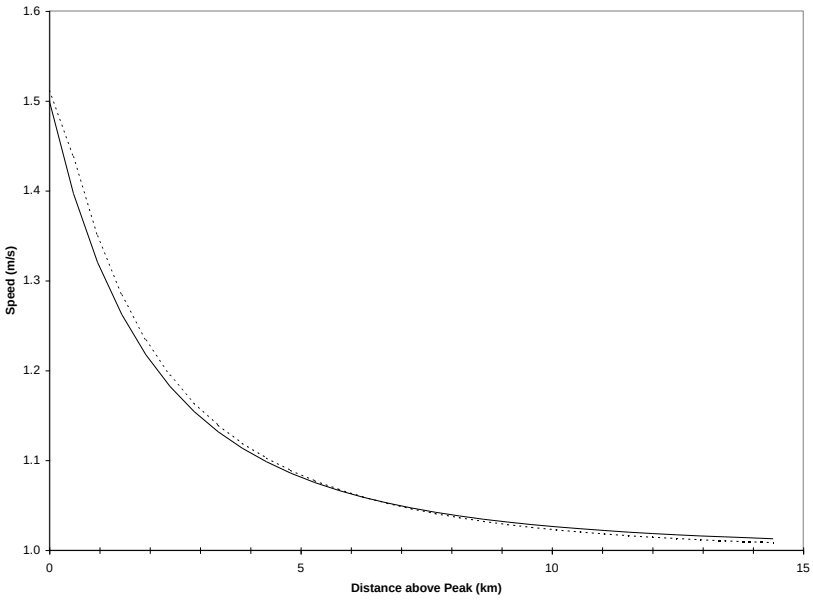

Figure 3: Vertical wind speed over a hemispherical mountain as a function of distance above the peak. (MILTWAM results are dotted. Analytic solution results are solid.)

b. Test Case 2: Half-Cylinder Mountain

The second test case for geometric terrain is a half-cylinder mountain with a radius of 6 km. The cylinder is laying on its side with long axis in the north-south direction. The computational grid is 49 by 49 km, with a grid spacing of 1 km. The model top is at 21 km, with 22 layers. An open boundary condition is used at the top so that the results could be compared with the analytic solution. The free-stream speed is 1 m/s in the x-direction.

Figure 4 shows the near-surface wind speed as a function of along wind distance from the center of the peak. According to MILTWAM, the maximum speed on the top of the cylinder is 1.8 m/s, as compared to 2 m/s for the analytic solution. At the stagnation points, where the analytic results are zero, MILTWAM gives 0.4 m/s. Again, the two curves agree very well at

distances beyond 6 km. Similarly, in Figure 5, for the vertical wind speed as a function of distance above the peak of the cylinder, the maximum deviation is about 10%.

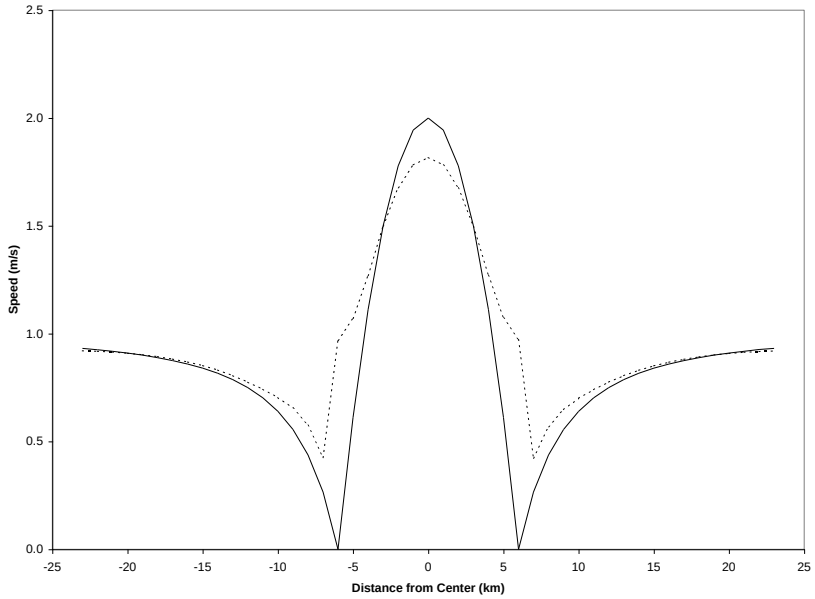

Figure 4: Surface wind speed over a half cylinder mountain as a function of along wind distance. (MILTWAM results are dotted. Analytic solution results are solid.)

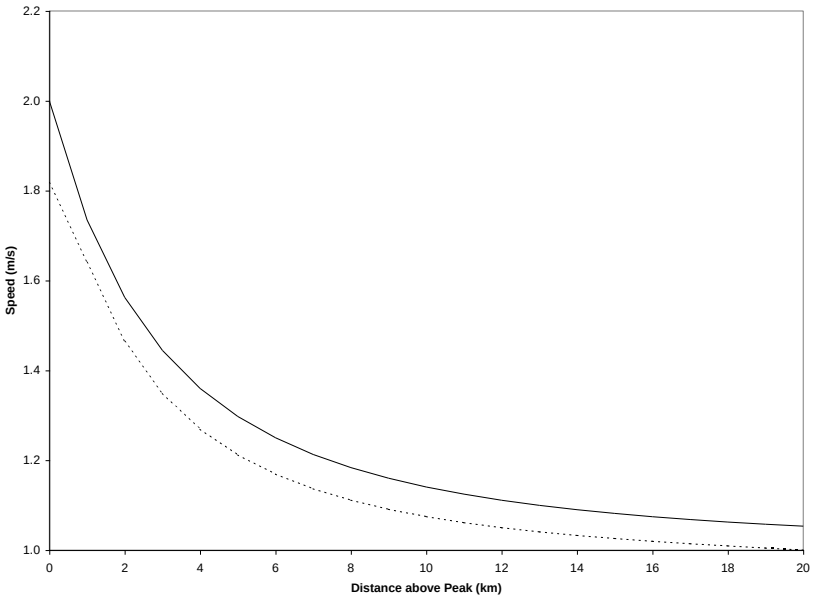

Figure 5: Vertical wind speed over a half cylinder mountain as a function of distance above the peak. (MILTWAM results are dotted. Analytic solution results are solid.)

c. Test Case 3: Cylinder Mountain

The third test case was run to compare the results of the two-dimensional component of MILTWAM with the analytic solution for flow around a cylinder. The terrain consists of a cylinder that stands vertically and has a radius of 10.5 km. The heights of the cylinder and the mixing layer are both 1000 m so that the cylinder extends through the entire mixing layer. This test case uses a 97 by 97 km computational grid with a grid spacing of 1 km. The free-stream velocity is 1 m/s from the east.

Figure 6 shows the wind speed as a function of along wind distance from the center of the cylinder mountain. Figure 7 shows the wind speed as a function of cross-wind distance from the center of the cylinder mountain. MILTWAM agrees excellently with the analytic solution. Figure

8 shows wind vectors near the cylinder based on MILTWAM and the analytic results. There is no discernible difference in this example, except in a small zone near the cylinder.

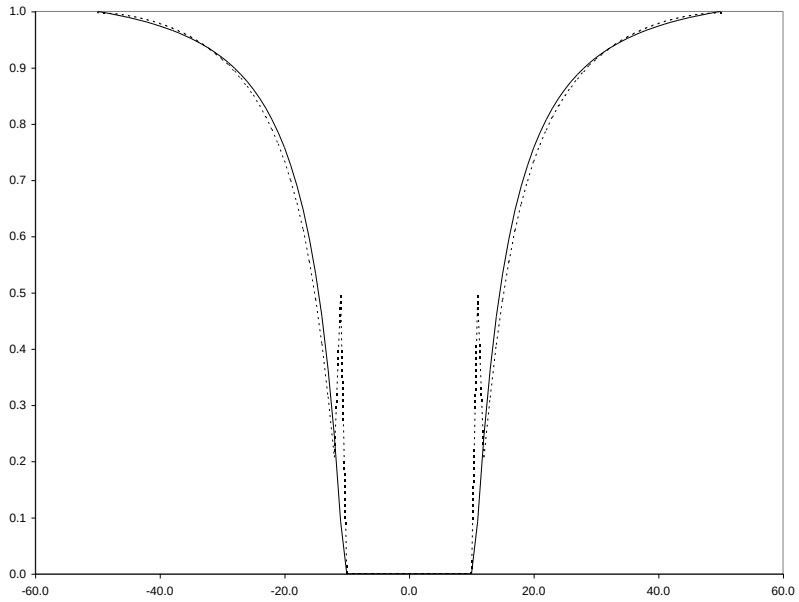

Figure 6: Wind speed near a cylinder mountain as a function of along wind distance from the center of the cylinder. (MILTWAM results are dotted. Analytic solution results are solid.)

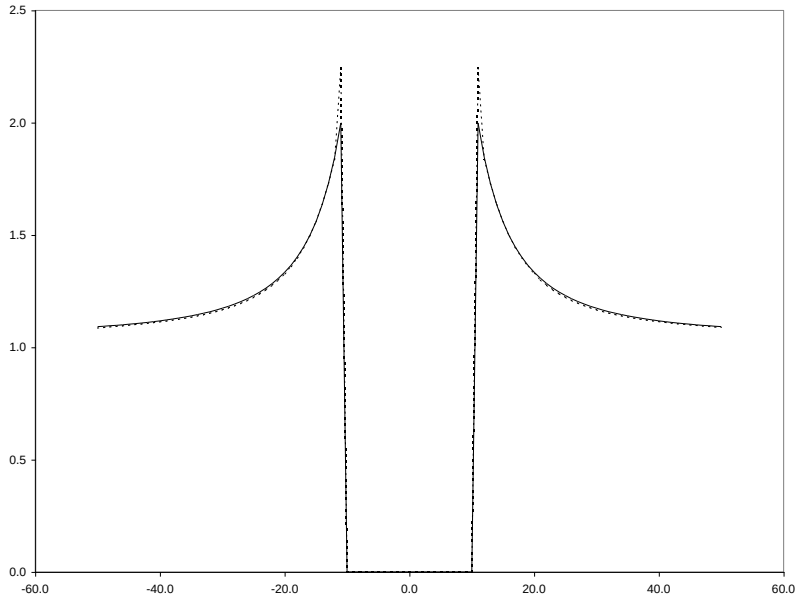

Figure 7: Wind speed near a cylinder mountain as a function of cross wind distance from the center of the cylinder. (MILTWAM results are dotted. Analytic solution results are solid.)

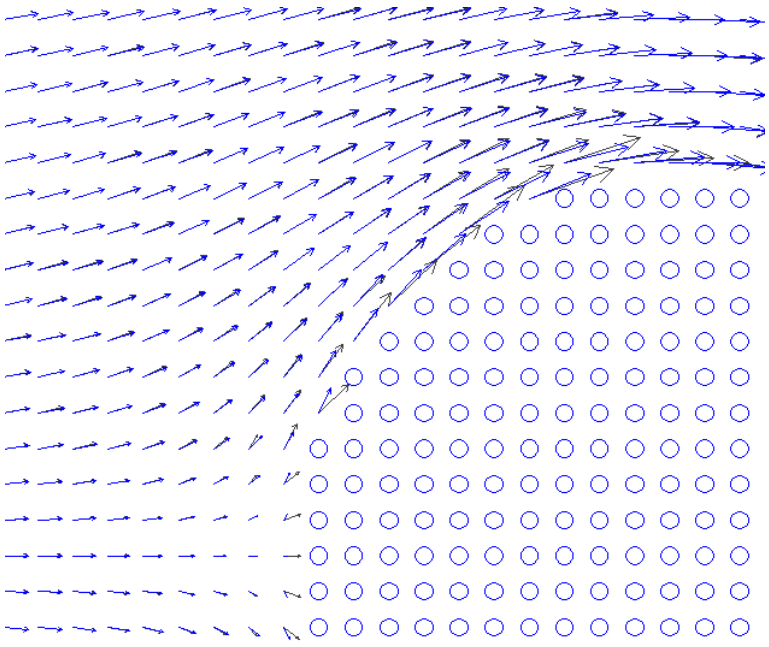

Figure 8: Wind vectors near a cylinder mountain. (MILTWAM results are black. Analytic results are blue.)

6. Results for Real Terrain

The largest CSEPP site is the Deseret Chemical Depot (DCD) located in Utah. As shown in Figure 9, this site is located in the Rush Valley and is bounded by two ridges: the Stansbury Mountains to the west and the Oouirrh Mountains to the east. The valley is mostly open at the north and southeastern ends. One low ridge (South Mountain) extends part way across the valley north of DCD, with a gap near Bauer. Another low ridge (the Thorpe Hills) runs across the southeastern end of the valley with gaps at Five Mile Pass and at Ten Mile Pass. The terrain in the model domain has a minimum elevation of 1265 m above sea level, a maximum elevation of 3252 m, and an average elevation of 1642 m. The elevation at the center of the chemical limited area at DCD is 1558 m.

Table 1 shows the average height of the mixing layer (Whitacre *et al*., 1987; Innovative Emergency Management, 1998) as a function of season and Pasquill stability class. These heights are given as vertical distance above the elevation of the chemical limited area. Note that the highest peak is 1694 m above the elevation of DCD. Thus, the two-dimensional component of MILTWAM is used for all values of the height of the mixing layer that are less than 1694 m.

Table 1: Average Heights of the Mixing Layer at Deseret Chemical Depot (DCD)

	A	B	C	D	E	F
Winter	540	540	**377**	215	100	**50**
Fall	**1470**	**1470**	**845**	220	100	80
Spring	**2310**	**2310**	1277	245	**150**	100
Summer	**3625**	**3625**	1892	200	100	80

Figure 10 through Figure 16 show the wind fields produced by MILTWAM for several mixing layer heights (shown in bold type in Table 1). All of the plots in this figure were produced using a single wind value of 1 m/s from 150 degrees at the center of the DCD chemical limited area. The blue vectors at the centers of Figure 9 through Figure 16 show this wind value.

A Note to Reviewers:

The left side of each panel in Figure 10 was produced by MILTWAM as it runs in D2-Puff. The plots show wind vectors. An IEM program called TerrTest produced the right side. TerrTest is a simple version of the 2D part of MILTWAM. The dashed curves are streamlines. We have included these panels because the streamlines make it easier to see the flow patterns and to evaluate the effect of the flow on plume transport. We are currently adding streamline drawing to D2-Puff. When this is done, only the D2-Puff output will be shown in this paper.

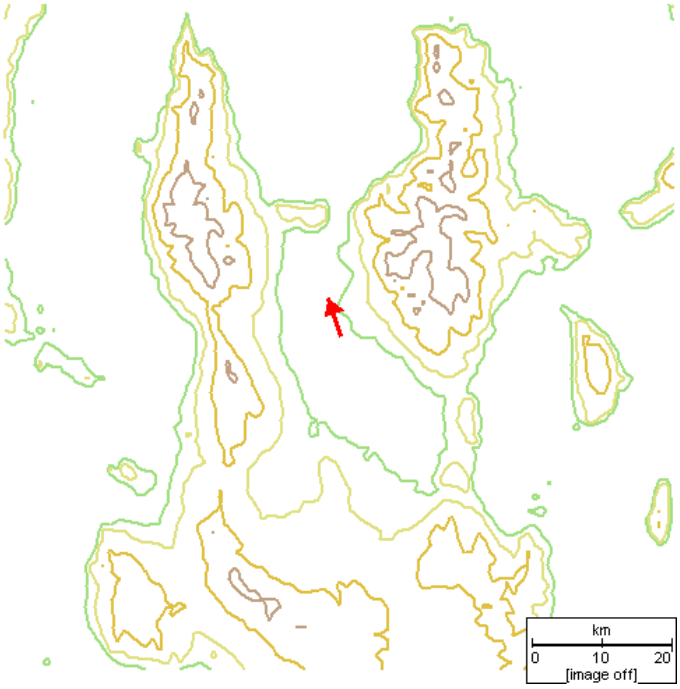

Figure 9: Terrain elevation in the vicinity of the Deseret Chemical Depot.

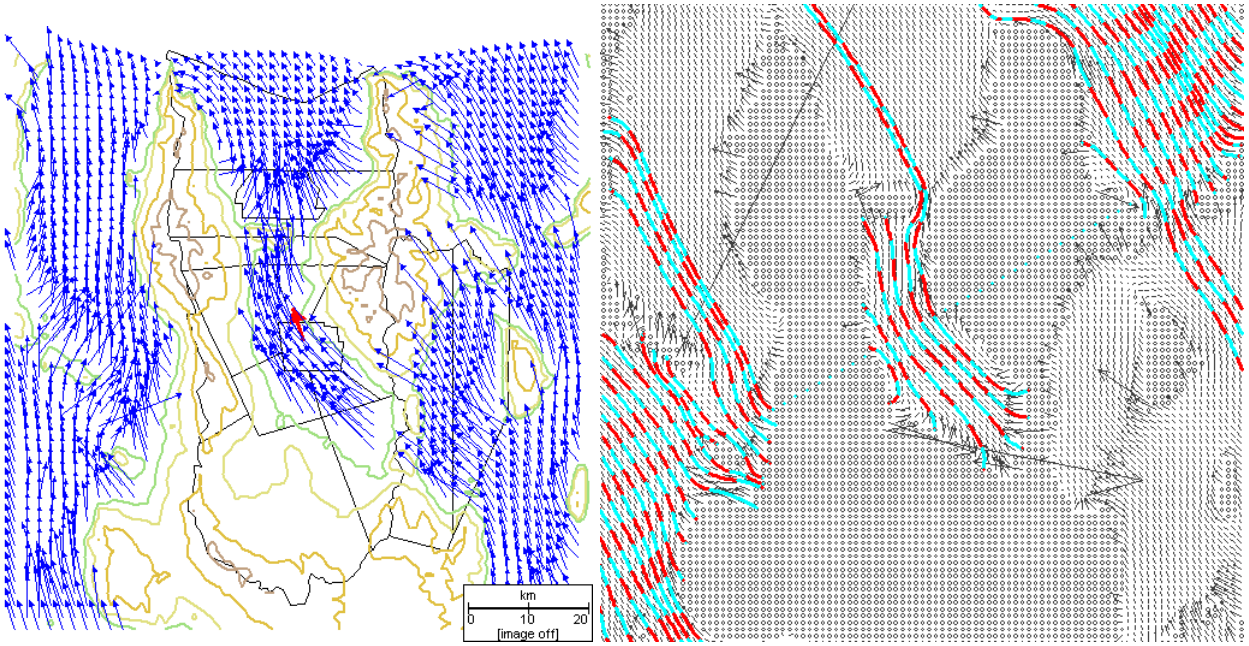

Figure 10: Winds in the vicinity of the Deseret Chemical Depot for a height of the mixing layer of 50 m.

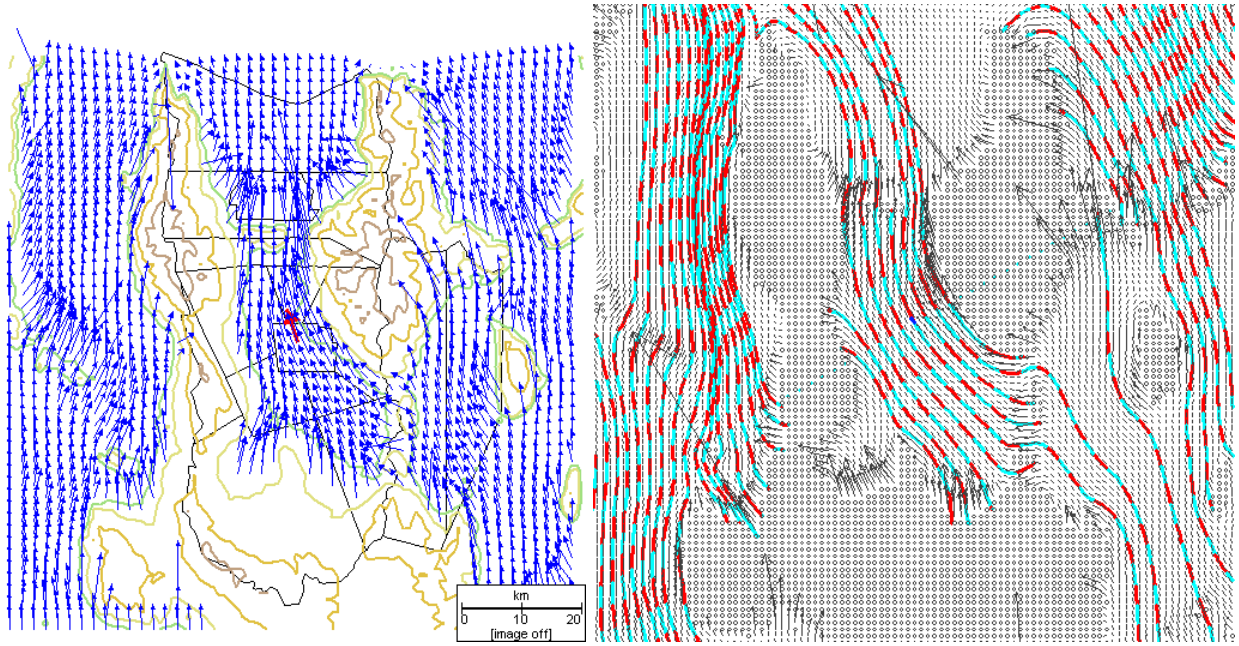

Figure 11: Winds in the vicinity of the Deseret Chemical Depot for a height of the mixing layer of 150 m.

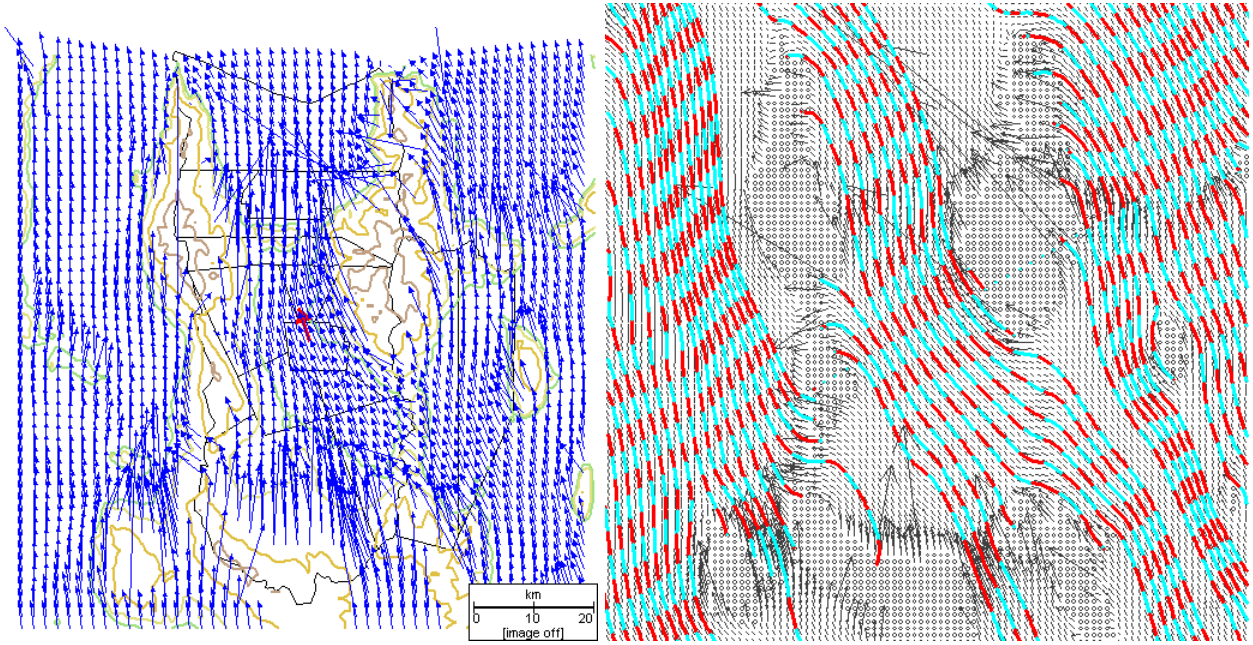

Figure 12: Winds in the vicinity of the Deseret Chemical Depot for a height of the mixing layer of 377 m.

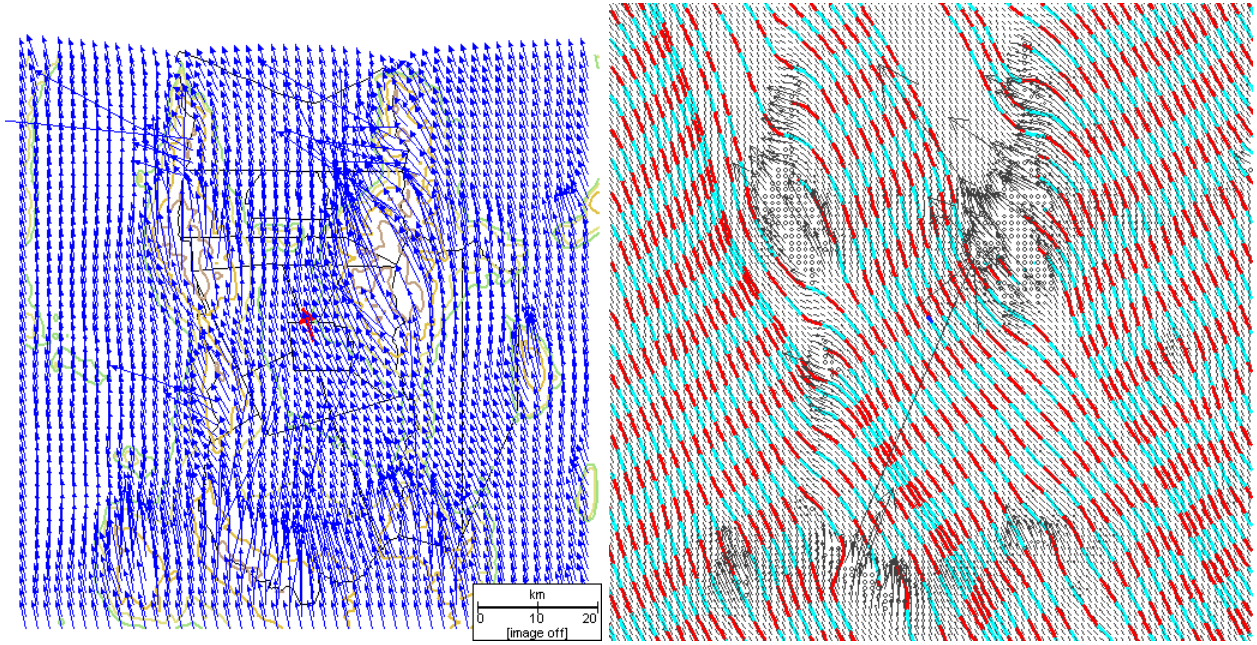

Figure 13: Winds in the vicinity of the Deseret Chemical Depot for a height of the mixing layer of 845 m.

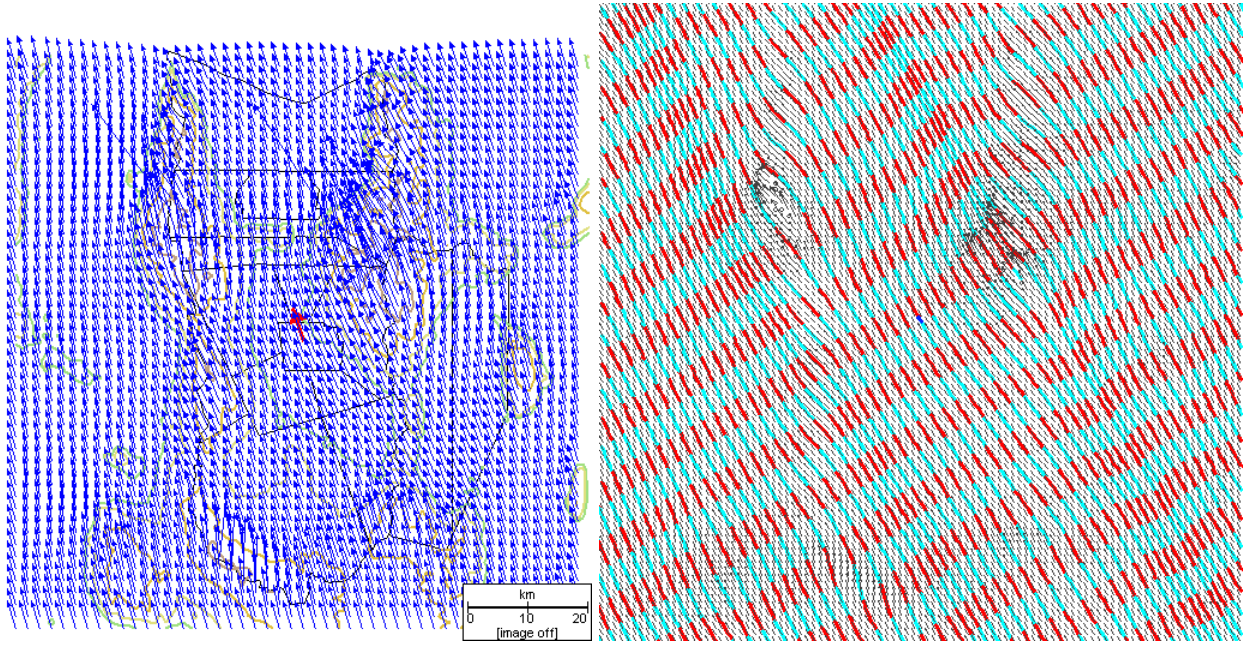

Figure 14: Winds in the vicinity of the Deseret Chemical Depot for a height of the mixing layer of 1470 m.

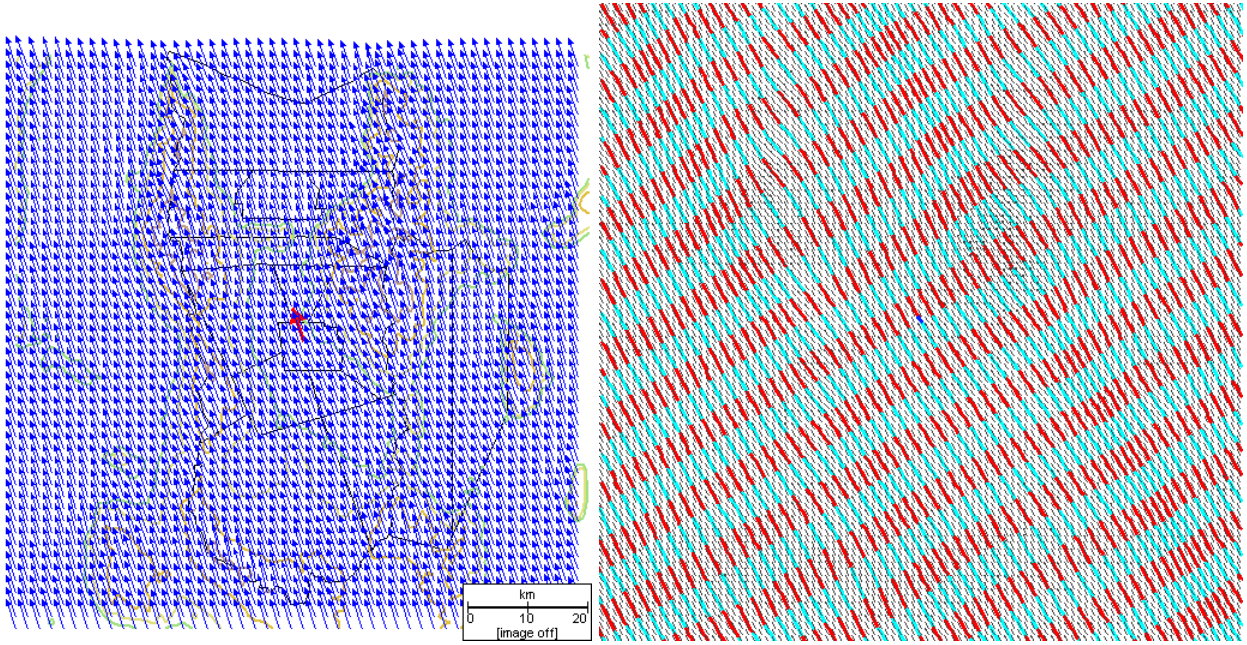

Figure 15: Winds in the vicinity of the Deseret Chemical Depot for a height of the mixing layer of 2310 m.

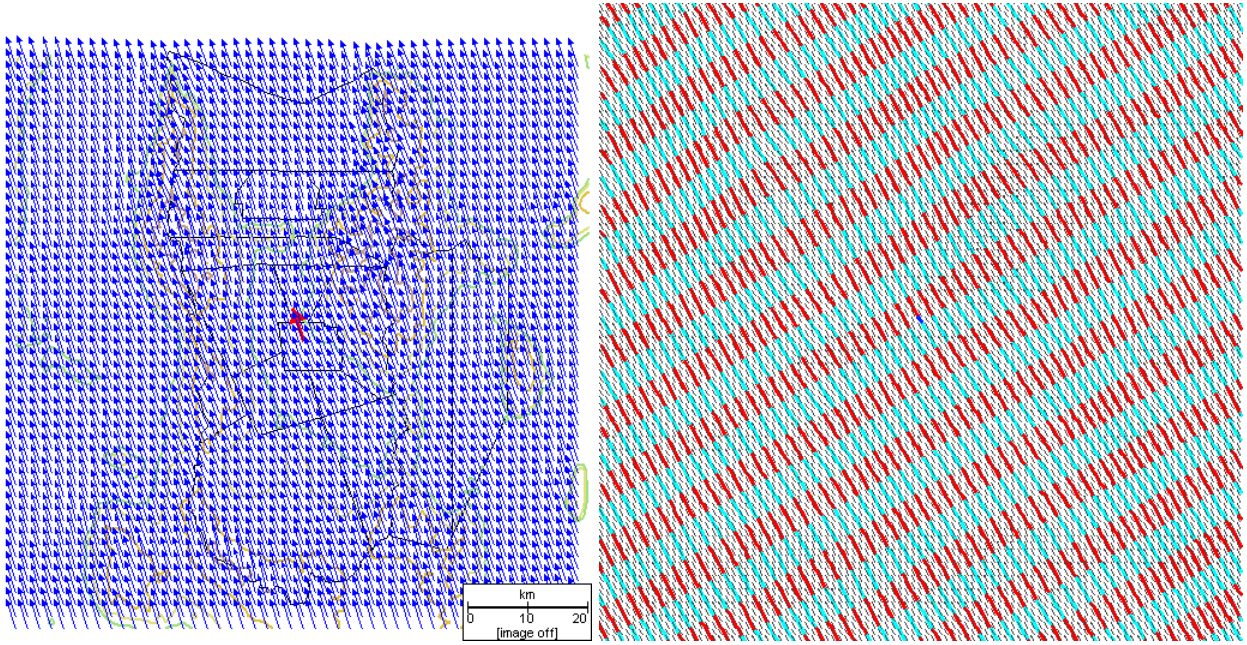

Figure 16: Winds in the vicinity of the Deseret Chemical Depot for a height of the mixing layer of 3625 m.

The purpose of the series of plots shown in Figure 10 through Figure 16 is to show how the height of the mixing layer and the terrain interact to determine the wind field. The value of 50 m for the height of the mixing layer occurs during very stable conditions. This height corresponds to the average mixing layer height during F stability in winter at DCD. In this case, the terrain is essentially a basin surrounding DCD. The only outlet for the wind is through the small gap in the ridge to the north. Most of the streamlines in the basin remain within the basin. When the height of the mixing layer is 150 m (Figure 11), the terrain functions more as a valley. This height corresponds to the average mixing layer height during E stability in spring at DCD. Streamlines are able to enter the valley through several gaps in the ridge to the southeast and to exit the valley over most of the low ridge to the north. All of the streamline shows considerable deflection around the terrain and the speed accelerates through narrow regions.

In Figure 12 the height of the mixing layer is 377 m, and the air is free to flow over the ridges at both ends of the valley. This height corresponds to the average mixing layer height during C stability in winter at DCD. The largest terrain features continue to channel the flow, and in some cases block the flow. Lower features do not block the flow but do deflect and accelerate it. For instance, higher wind speeds can be seen over the low ridges at the ends of the valley.

For a height of the mixing layer of 845 m (Figure 13), air can cross the ridges to the east and west at several locations, and the pattern is more likely to flow around the highest peaks than to flow trapped in a valley. This height corresponds to the average mixing layer height during C stability in fall at DCD. When the height of the mixing layer is 1470 (Figure 14) the mixing layer top is not much below the tops of the highest peaks. This height corresponds to the average mixing layer height during A or B stability in fall at DCD. Only two peaks protrude from the

mixing layer. Very little blockage of the flow occurs, and the air is readily able to flow around the hills.

Figure 15 shows a mixing layer height of 2310 m. This height corresponds to the average mixing layer height during A or B stability in spring at DCD. Figure 16 shows a mixing layer height of 3625 m. This height corresponds to the average mixing layer height during A or B stability in summer at DCD. These heights are above the highest terrain. Thus, the three-dimensional model equations are used in MILTWAM. The winds shown in these panels are the near-surface values. In these cases, variations in wind speed and direction are quite small.

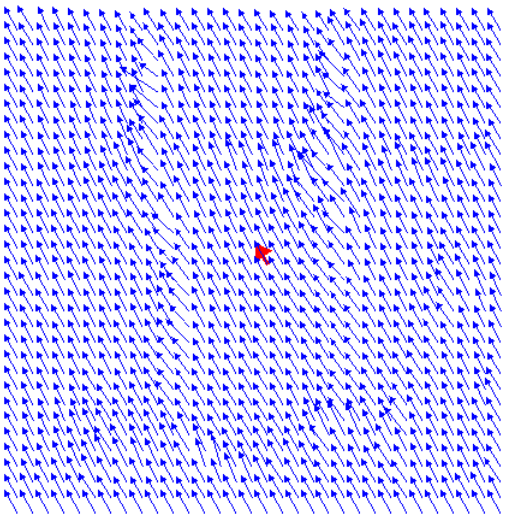

Figure 17: Winds in the vicinity of the Deseret Chemical Depot based on NUATMOS.

Figure 17 shows the flow that would be produced by NUATMOS for D or F stability for any season. The figure was obtained by running MILTWAM with a wind of 1 m/s from 150 degrees, a height of the top level of the model set to 3700 m, an *open* upper boundary condition, and a value of 0.031 for α^2. Comparing this figure with Figure 10 and Figure 11 shows that

MILTWAM produces much larger adjustments to the winds than NUATMOS, and that the MILTWAM winds have a much greater tendancy to flow around the terrain.

It should be noted that the top of the model in Figure 17 is high enough above the terrain that the height of the model top and the use of an open boundary condition at the model top do not significantly effect the wind field. Thus the value α^2 and the observed wind speed and direction are the only factors in determining the flow.

7. Summary and Conclusions

MILTWAM is a mass-consistent model for airflow over complex terrain. It is based on the NUTAMOS model, though it includes several changes. The top of the mixing layer is explicitly included in the model and functions as a non-porous lid. It is the major factor in limiting vertical motions. MILTWAM makes a three-dimensional wind adjustment when the highest terrain is within the mixing layer and a two-dimensional adjustment when the terrain protrudes above the mixing layer. MILTWAM produces flows showing considerable deflection and acceleration around the terrain, even when only one observation or a few observations are available. The model is fast and can be run on a PC in a few seconds; it is therefore well suited for use in an emergency response dispersion model.

ACKNOWLEDGEMENTS

We thank Dr. D. G. Ross, Center for Applied Mathematical Modeling, Monash University, Australia, for providing us with the NUATMOS input and output data for comparison study and for useful theoretical discussions.

REFERENCES

Briggs, William L., 1987: *A Multi-grid Tutorial*. SIAM publication, 90 pp.

Burch, S. F., and F. Ravenscroft, 1992: Computer Modelling the UK Wind Energy Resource: Final Overview Rport. Technical Report ETSU WN 7055, AEA Industrial Technology, Harwell Laboratory, page numbers and whole address.

Cox, R. M., J. Sontowski, R. N. Fry, C. M. Dougherty, and T. J. Smith, 1998: Wind and Diffusion Modeling for Complex Terrain. *J. App. Met*., **37**, 996-1009.

Draxler, R. R., 1991: The accuracy of trajectories during ANATEX calculated using dynamic model analyses versus rawinsonde observations. *J. App. Met*, **30**, 1446-1467.

——, and G. D. Hess, 1998: An overview of the HYSPLIT_4 Modeling System for trajectories, dispersion, and deposition. *Australian Meteorological Magazine*, **47**, 295-308.

Innovative Emergency Management, 1998: D2-Puff 2.0.5 Reference Manual. IEM Tech. Rep. IEM/TEC98-029, 129 pp.

Lewellen, W. S., R. I. Sykes, and D. Oliver, 1982: The Evaluation of MATTHEW/ADPIC as a Real Time Dispersion Model. Prepared for U.S. Nuclear Regulatory Comm., NUREG/CR-2199 ARAP Rep. No.442, 125 pp.

Pennel, W. T., 1983: An Evaluation of the Role of Numerical Wind Field Models in Wind Turbine Siting. Batelle Memorial Institute Tech. Rep. PNL-SA-11129, Batelle Memorial Institute, Pacific Northwest Laboratory, Richland, Washington, page numbers and whole address.

Press, W. H., S. A. Teukolsky, W. T. Vetterling, and B. P. Flannery, 1997: *Numerical Recipes in C, The Art of Scientific Computing.* 2nd ed. Cambridge University Press, 994 pp.

Ratto, C. F., R. Festa, C. Romeo, O. A. Frumento, and M. Galluzzi, 1994: Mass-Consistent Models for Wind Fields over Complex Terrain: The State of the Art. *Environmental Software*, **9**, 247-268.

Robe, F. R., and J. S. Scire, 1998: Combining Mesoscale Prognostic and Diagnostic Wind Models: a practical approach for air quality applications in complex terrain. *Proc. 10th Conference on Air Pollution Met.,* Phoenix, Arizona, Amer. Meteor. Soc., 223-226.

Ross, D. G., I. N. Smith, P.C. Manis, and D. G. Fox, 1988: Diagnostic Wind Field Modeling for Complex Terrain: Model Development and Testing. *J. App. Met*., **27**, 785-796.

——, and G. S. Lorimer, J. Ciolek, and D. G. Fox, 1993: Development and Evaluation of a Wind-Field Model for Emergency Preparedness in Complex Terrain. Preprints, *86th Annual Meeting and Exhibition*, Denver, Colorado, Air and Waste Management Association, 1-13.

Sasaki, Y. 1958: An objective analysis based on the variational method. *J. Meteor. Soc. Japan*, **36**, 77-78.

Selvam, R. P. and K. S. Rao, 1996: WINDFCT: A mass consistent wind field model for complex terrain. *Proc. 9th Joint Conference on Air Pollution Meteorology*, Atlanta, Georgia, Amer. Meteor. Soc., 397-400.

Sherman, Christine A., 1978: A Mass-Consistent Model for Wind-Fields over Complex Terrain. *J. App. Met.*, **17**, 312-319.

U.S. Environmental Protection Agency, 1995: A User's Guide for the CALMET Meteorological Model. U.S. EPA Tech. Rep. EPA-454/B-95-002, 345 pp.

Whitacre, C.G., J.H. Griner III, M. Myirski, and D.W. Sloop, 1987: Personal Computer Program for Chemical Hazard Prediction (D2PC). Chemical Research, Development & Engineering Center Tech. Rep. CRDEC-TR-87021, 152 pp. [Available from Defense Technical Information Center, 8725 Kingman Road Suite 0944, Fort Belvoir, Virgina, 22060-6218, AD Number: A177622.]